Article:
Farmer, M.A.H. orcid.org/0009-0008-9645-6921, Musa, O.M. and Armes, S.P. orcid.org/0000-0002-8289-6351 (2024) Jeffamine-based diblock copolymer nanoparticles via reverse sequence polymerization-induced self-assembly in aqueous media. Polymer, 310. 127474. ISSN 0032-3861

https://doi.org/10.1016/j.polymer.2024.127474

Polymer 310 (2024) 127474

Contents lists available at ScienceDirect

Polymer

journal homepage: www.elsevier.com/locate/polymer

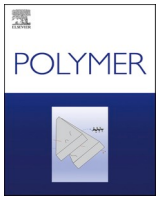

Jeffamine-based diblock copolymer nanoparticles via *reverse sequence* polymerization-induced self-assembly in aqueous media

Matthew A.H. Farmer [a,**], Osama M. Musa [b], Steven P. Armes [a,*]

[a] Dainton Building, Department of Chemistry, University of Sheffield, Brook Hill, Sheffield, South Yorkshire, S3 7HF, UK
[b] Ashland Specialty Ingredients, 1005 US 202/206, Bridgewater, NJ, 08807, USA

A B S T R A C T

Jeffamines® are commercially available amine-capped poly (alkylene oxides) that have been used for various applications. In this study, a weakly hydrophobic monoamine-capped propylene oxide-rich Jeffamine® (M2005) is derivatized to introduce a trithiocarbonate end-group via amidation. This precursor is then dissolved using N,N′-dimethylacrylamide (DMAC), 2-(N-acryloyloxy)ethyl pyrrolidone (NAEP) or N-acryloylmorpholine (NAM) as a co-solvent to produce a concentrated aqueous reaction mixture containing 20 % w/w water. Subsequently, reversible addition-fragmentation chain transfer (RAFT) polymerization is used to prepare Jeffamine®-core diblock copolymer nanoparticles by reverse sequence polymerization-induced self-assembly (PISA). At intermediate conversion, additional degassed water is added and each polymerization continues to almost full conversion (>99 %) within 4 h at 60 °C, resulting in a 10–20 % w/w aqueous dispersion of sterically-stabilized Jeffamine®-core nanoparticles. Efficient chain extension of the Jeffamine® precursor is achieved in most cases and relatively narrow molecular weight distributions are obtained ($M_w/M_n < 1.30$) as judged by GPC analysis. Transmission electron microscopy studies confirm a polydisperse spherical morphology and dynamic light scattering studies report hydrodynamic diameters ranging from 145 to 312 nm. Finally, aqueous electrophoresis studies indicate essentially neutral nanoparticles over a wide range of solution pH, as expected for the three types of non-ionic steric stabilizer chains selected for this study.

1. Introduction

Polymerization-induced self-assembly (PISA) is a well-known platform technology that enables the efficient synthesis of concentrated colloidal dispersions of block copolymer nanoparticles [1–7]. In the case of aqueous PISA formulations, a water-soluble homopolymer is first prepared using reversible addition-fragmentation chain transfer (RAFT) polymerization [8], atom transfer radical polymerization (ATRP) [9] or nitroxide-mediated polymerization (NMP) [10]. Subsequently, this precursor is chain-extended in aqueous media using a suitable monomer such that the growing block becomes hydrophobic at some critical degree of polymerization (DP), which leads to *in situ* self-assembly to form nascent nanoparticles [11,12]. The polymerization continues within monomer-swollen nanoparticles until full monomer conversion is achieved. The most common final copolymer morphology is spheres but highly anisotropic worms or polydisperse vesicles can also be prepared [13–16]. Compared to traditional post-polymerization processing routes to block copolymer nanoparticles, PISA is much more efficient and process-intensive [17–21]. Moreover, PISA can also be conducted in non-aqueous media [22–28]. However, PISA formulations typically involve vinyl monomers, which invariably produce non-degradable, environmentally-persistent polymers that do not address growing concerns regarding the global problem of microplastic pollution [29–31]. Hence many research groups have recently developed new PISA formulations to produce degradable block copolymer nanoparticles [32–41]. Primarily, this has involved statistical copolymerization of cyclic comonomers with vinyl monomers to introduce cleavable (thio) ester bonds into the polymer backbone [32–35]. In addition, the ring-opening of *N*-carboxyanhydrides (NCAs) has been conducted in either water or THF to produce polypeptide-based block copolymer nanoparticles [36,37,40].

Recently, we have developed a new approach to hydrolytically-degradable nanoparticles via PISA [38]. This formulation involves using a hydrophilic vinyl monomer (*N,N′*-dimethylacrylamide, DMAC) to solubilize a hydrophobic trithiocarbonate-capped poly (ε-caprolactone) (PCL) precursor in concentrated aqueous solution at 80°C. Subsequently, the RAFT polymerization of DMAC is conducted and, at a convenient intermediate DMAC conversion, the reaction mixture is diluted with deoxygenated water and *in situ* self-assembly occurs to produce nascent nanoparticles. The polymerization is allowed to continue, eventually resulting in the formation of hydrolytically-degradable PCL-PDMAC nanoparticles [37]. Since the

* Corresponding author.
** Corresponding author.
E-mail addresses: mahfarmer1@sheffield.ac.uk (M.A.H. Farmer), s.p.armes@sheffield.ac.uk (S.P. Armes).

https://doi.org/10.1016/j.polymer.2024.127474
Received 25 June 2024; Received in revised form 5 August 2024; Accepted 6 August 2024
Available online 8 August 2024

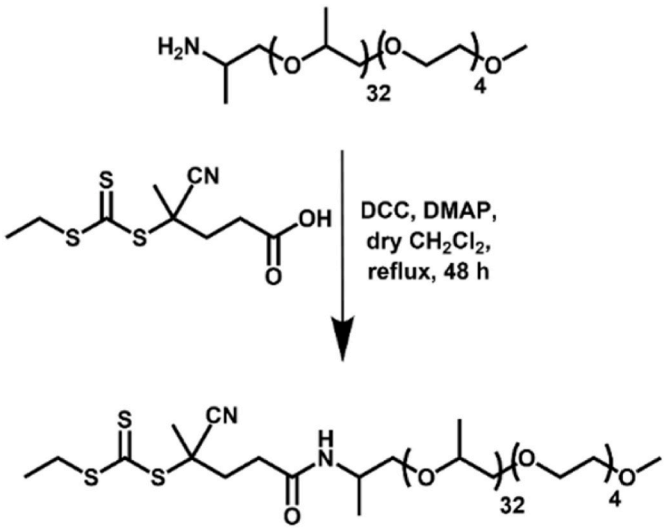

Scheme 1. Amidation of a primary amine-capped Jeffamine® M − 2005 precursor using a carboxylic acid-functionalized RAFT agent (CEPA) and a DCC/DMAP catalyst in dry dichloromethane.

hydrophobic block is prepared before the hydrophilic block, we use the recently introduced term 'reverse sequence PISA' to describe such syntheses [38,41–43].

Herein we seek to expand such reverse sequence PISA formulations by evaluating several hydrophilic vinyl monomers and a hydrophobic precursor. More specifically, Jeffamines® (Huntsman Chemicals, The Netherlands) are a class of commercially available amine-functionalized poly (alkylene oxides) comprising propylene oxide (PO) and ethylene oxide (EO) comonomers [44–46]. In principle, placing an amide bond at the block junction is likely to reduce the potential hydrolytic degradability of the overall diblock copolymer. However, this is not the focus of the current study. Instead, we exploit the relatively high solubility of the Jeffamine® M − 2005 precursor in various vinyl monomers to examine the effect of varying the nature of the hydrophilic block, which has so far been mainly restricted to PDMAC [38,41,47].

Accordingly, a weakly hydrophobic trithiocarbonate-capped Jeffamine® precursor (M − 2005) is prepared via amidation (see Scheme 1) and then chain-extended via RAFT polymerization using various hydrophilic vinyl monomers in turn, e.g. DMAC, *N*-(2-acryloyloxy)ethyl pyrrolidone (NAEP), or *N*-acryloyl morpholine (NAM), see Scheme 2. Such polymerizations are conducted initially in concentrated aqueous solution prior to dilution with deoxygenated water to 10–20 % w/w solids at a suitable intermediate conversion. The resulting diblock copolymer chains/nanoparticles are analyzed using ^{1}H NMR spectroscopy, gel permeation chromatography (GPC), transmission electron microscopy (TEM), dynamic light scattering (DLS) and aqueous electrophoresis.

2. Experimental

2.1. Materials

Glycerol monomethacrylate (GMA) was donated by GEO Specialty Chemicals (Hythe, UK). 2-(*N*-Acryloyloxy)ethyl pyrrolidone (NAEP; 95 %) and 2-(*N*-methacryloyloxy)ethyl pyrrolidone (NMEP; 98 %) were donated by Ashland Specialty Ingredients (Cherry Hill, NJ, USA). *N,N′*-Dimethylacrylamide (DMAC; 99 %), *N*-hydroxyethyl acrylate (HEA), *N*-hydroxyethyl acrylamide (HEAC), *N*-acryloylmorpholine (NAM; 97 %), anhydrous magnesium sulfate, lithium bromide, dichloromethane, 2,2′-azobis(2-methylpropionamidine) dihydrochloride (AIBA; 97 %), *N,N′*-dicyclohexylcarbodiimide (DCC; 99 %), deuterated chloroform (99.8 %) and *n*-hexane were purchased from Sigma Aldrich (Dorset, UK). 4-(Dimethylamino)pyridine (DMAP) was purchased from Alfa Aesar (Heysham, UK). Dimethylformamide (DMF) and triethylamine was purchased from VWR (Leicestershire, UK). Ethyl acetate, chloroform and methanol were purchased from Fisher Scientific (Loughborough, UK). Deuterated methanol (CD_3OD, 99.8 %) was purchased from Goss Scientific Instruments Ltd (Cheshire, UK). Unless otherwise stated, all reagents were used as received. The NAEP monomer was purified prior to use by diluting in chloroform and washing with 5 % aqueous Na_2CO_3,

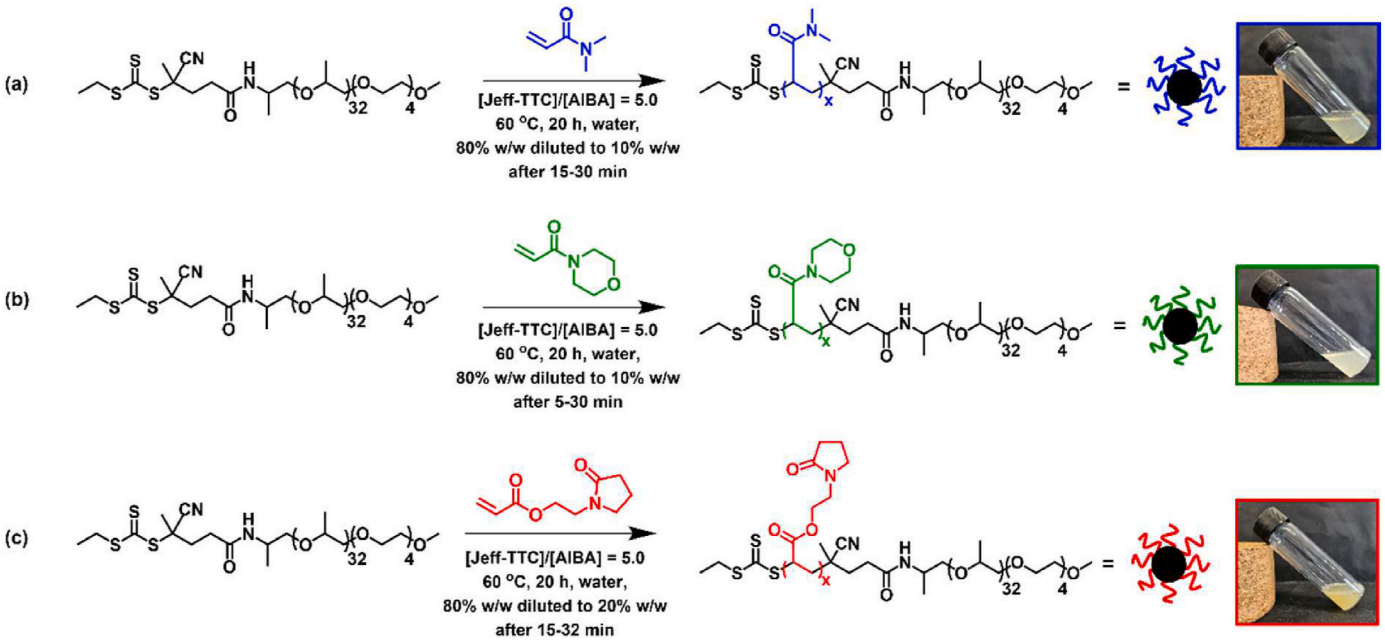

Scheme 2. RAFT polymerization of (a) DMAC, (b) NAM or (c) NAEP when using a Jeffamine®-based precursor conducted in concentrated aqueous solution (80 % w/w solids) at 60 °C, along with corresponding digital photographs to illustrate the physical appearance of the final aqueous copolymer dispersions when targeting a steric stabilizer DP of 120. At a suitable intermediate monomer conversion, dilution to 10–20 % w/w solids using deoxygenated water leads to *in situ* self-assembly of the amphiphilic block copolymer chains and the formation of sterically-stabilized diblock copolymer nanoparticles comprising Jeffamine® cores.

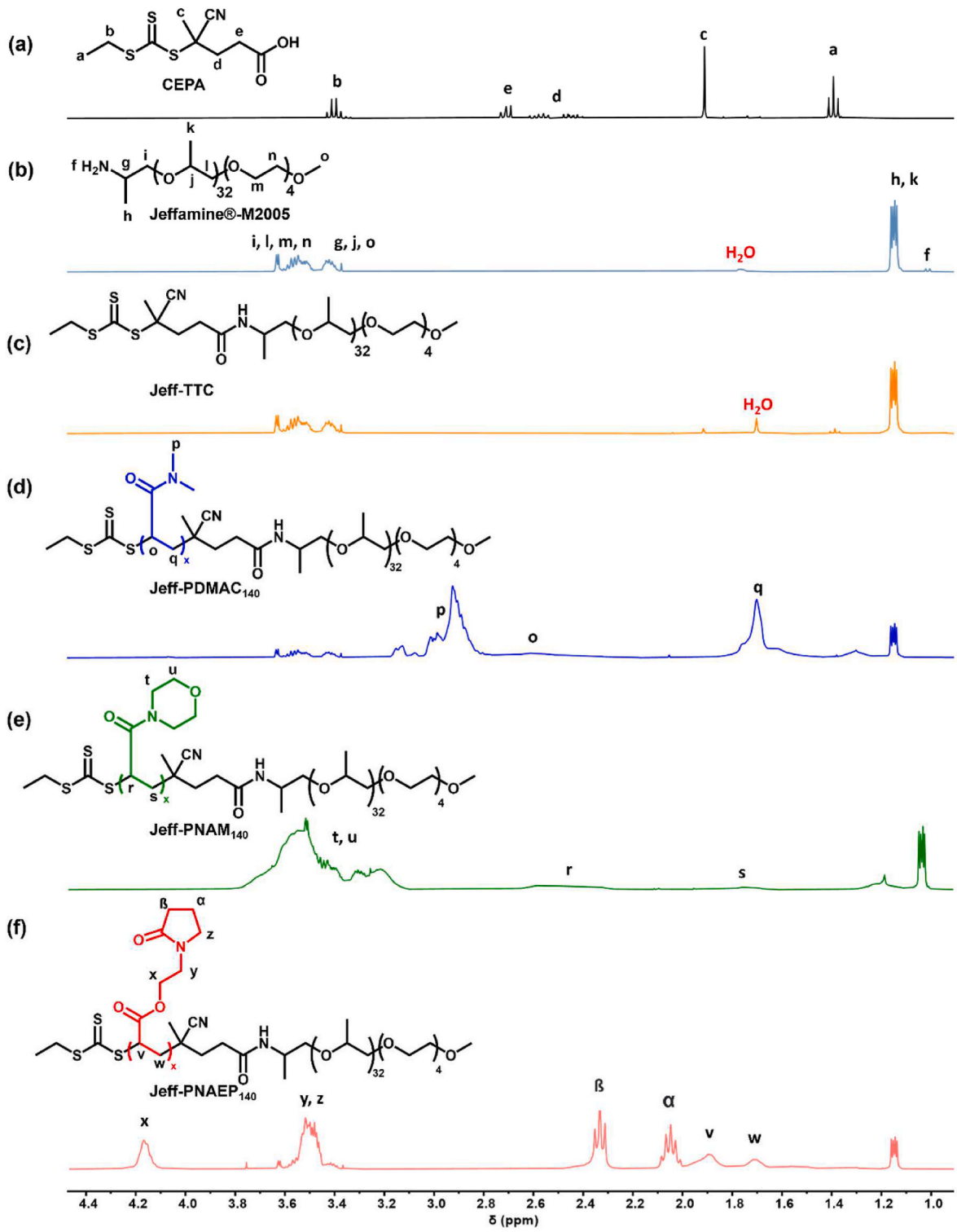

Fig. 1. ^{1}H NMR spectra ($CDCl_3$) recorded for (a) CEPA RAFT agent, (b) Jeffamine® M − 2005 precursor (denoted 'Jeff' hereafter), (c) the corresponding Jeff-TTC RAFT agent, (d) Jeff-PDMAC$_{140}$ diblock copolymer, (e) Jeff-PNAM$_{140}$ diblock copolymer and (f) Jeff-PNAEP$_{140}$ diblock copolymer.

saturated aqueous NaCl, and deionized water. Jeffamine® M − 2005 was donated by Huntsman Corporation (Rotterdam, The Netherlands). The mean degree of polymerization of the Jeffamine® M − 2005 was determined using ^{1}H NMR spectroscopy (see Fig. S1). The 4-cyano-4-(ethylsulfanylthiocarbonyl)sulfanyl pentanoic acid (CEPA) RAFT agent was prepared in 82 % yield according to a literature protocol [48]. For the synthesis of the trithiocarbonate-capped Jeffamine® precursor (denoted hereafter as 'Jeff-TTC'), anhydrous dichloromethane was obtained from an in-house Grubbs purification solvent system. Deionized water was obtained from an Elgastat Option 3 A water purification unit (resistivity = 15 MΩ cm) and used for all aqueous formulations.

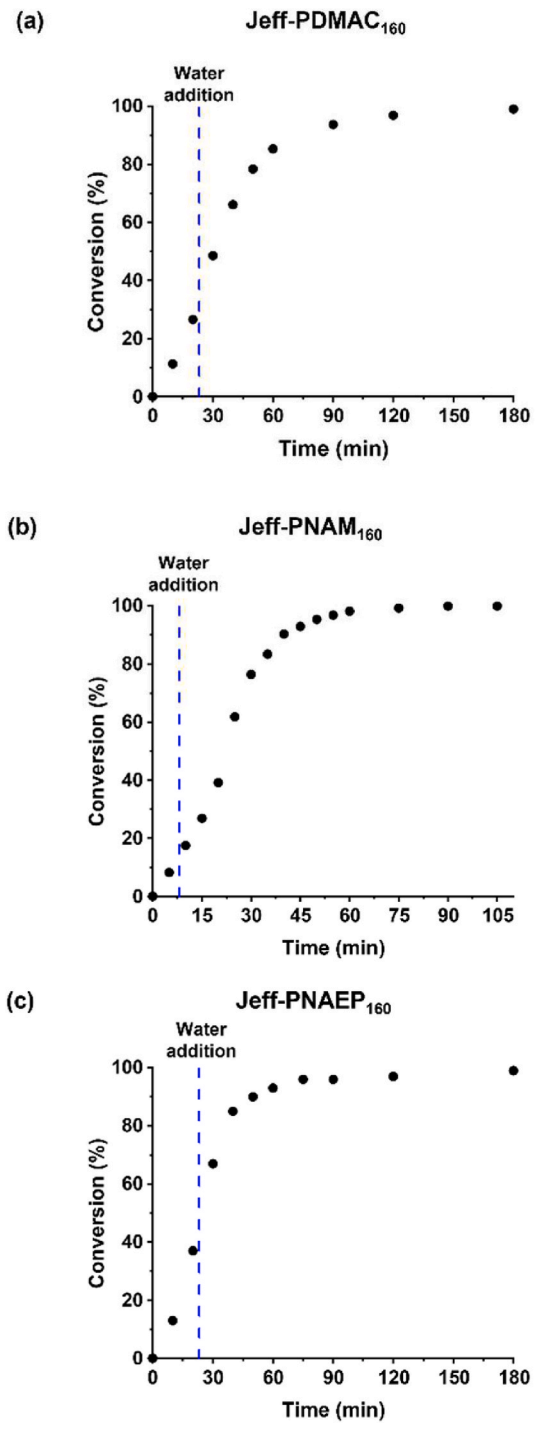

Fig. 2. Conversion vs. time curves obtained by ^{1}H NMR spectroscopy for the reverse sequence aqueous PISA synthesis of (a) Jeff-PDMAC$_{160}$ nanoparticles, (b) Jeff-PNAM$_{160}$ nanoparticles and (c) Jeff-PNAEP$_{160}$ nanoparticles at 60°C. Initially, these RAFT polymerizations were conducted at 80 % w/w solids, with subsequent dilution to 10 % w/w solids (or 20 % w/w solids for the Jeff-PNAEP$_{160}$ nanoparticles) using deoxygenated water. Intermediate conversions were estimated by interpolation and corresponded to (a) 38 %, (b) 16 % and (c) 45 %. Final vinyl monomer conversions of more than 99 % were achieved in all cases. Conditions: [Jeff-TTC]/[AIBA] molar ratio = 5.0.

2.2. Characterization techniques

^{1}H NMR Spectroscopy. Samples were diluted with $CDCl_3$ prior to NMR analysis. For aqueous dispersions, each sample was dried with anhydrous magnesium sulfate and filtered prior to $CDCl_3$ addition. For kinetic studies, all samples were diluted with CD_3OD. To calculate intermediate conversions, the integrated vinyl proton signals for each hydrophilic monomer at approximately 5.6–6.8 ppm were compared to the integrated signal at 1.15 ppm assigned to the pendent methyl group of the Jeffamine® precursor. ^{1}H NMR spectra were recorded using a 400 MHz Bruker Avance-400 spectrometer operating at 298 K; 16 scans were averaged per spectrum.

Gel Permeation Chromatography (GPC). GPC analysis of Jeff-PDMAC$_x$ and Jeff-PNAEP$_x$ copolymers was performed at 60°C using DMF eluent containing 10 mM LiBr at a flow rate of 1.0 mL min^{-1}. The GPC set-up comprised an Agilent 1260 Infinity GPC system equipped with two Agilent PL-gel 5 μm Mixed-C columns, a guard column, a differential refractive index detector and a UV–visible detector operating at 305 nm. GPC analysis of Jeff-PNAM$_x$ copolymers was performed at 35°C using chloroform eluent containing 0.25 % v/v triethylamine. Each copolymer solution was diluted to 1.0 % w/w using the relevant eluent prior to GPC analysis. For Jeff-PNAM$_x$ samples in chloroform, residual water was removed by drying with anhydrous magnesium sulfate followed by filtration. In all cases, chromatograms were analyzed using Agilent GPC/SEC software to determine the number-average molecular weight (M_n), the weight-average molecular weight (M_w) and dispersity (M_w/M_n). A series of twelve near-monodisperse poly(methyl methacrylate) standards with M_p values ranging from 800 g mol^{-1} to 2 200 000 g mol^{-1} were used for calibration.

Dynamic Light Scattering (DLS). Aqueous dispersions of copolymer nanoparticles were diluted to 1.0 % w/w using deionized water and equilibrated for 5 min prior to DLS analysis. DLS analysis was performed at 20°C using a Malvern Instruments Zetasizer Nano ZS instrument fitted with a 4 mW He–Ne laser (λ = 633 nm). An avalanche photodiode detector collected scattered light at an angle of 173°. Data obtained from three consecutive runs consisting of ten measurements per run were averaged to calculate the z-average particle diameter (D_z) and the polydispersity index (PDI).

Transmission Electron Microscopy (TEM). Nanoparticles were imaged by placing a 10 μL droplet of a 1.0 % w/w aqueous copolymer dispersion onto a copper/palladium grid (Agar Scientific, UK) that had been coated in-house with a thin film of amorphous carbon and exposed to plasma glow-discharge for 30 s to generate a hydrophilic surface. Each droplet was left for 1 min before blotting with filter paper to remove any excess. Subsequently, the nanoparticles were exposed to a 0.75 % w/v aqueous uranyl formate solution (negative stain) for 20 s. Again, excess solution was removed by blotted and the TEM grid was carefully dried with a vacuum hose. Imagining was performed with a FEI Tecnai Spirit TEM instrument operating at 80 kV and equipped with a Gatan 1kMS600 C W CCD camera. *ImageJ* software was used to estimate number-average particle diameters (based on the analysis of 50 nanoparticles per sample).

Aqueous Electrophoresis. Aqueous dispersions of copolymer nanoparticles were diluted to 1.0 % w/w using an aqueous solution of 1 mM KCl as a background electrolyte. In each case, the electrophoretic mobility was determined at 20 °C using a Malvern Instruments Zetasizer Nano ZS instrument and the Henry equation was used to calculate zeta potentials using the Smoluchowski approximation.

2.3. Experimental procedures

2.3.1. Synthesis of the Jeff-TTC precursor

Jeffamine® M − 2005 (5.00 g, 2.36 mmol), DMAP (0.05 g, 0.45 mmol), DCC (1.65 g, 7.99 mmol) and CEPA (1.05 g, 4.00 mmol) were weighed into four separate flame-dried glass vials. Each vial was sealed with a rubber septum and then dried in a vacuum oven for 2 h at 35°C. A minimal amount of dry dichloromethane was used to dissolve each reagent and the Jeffamine®, DMAP and CEPA solutions were transferred via syringe to a dry two-necked 100 mL round bottom flask fitted with a condenser, containing a magnetic stirrer bar, and sealed with rubber septa. This solution was cooled using an ice bath and the DCC solution

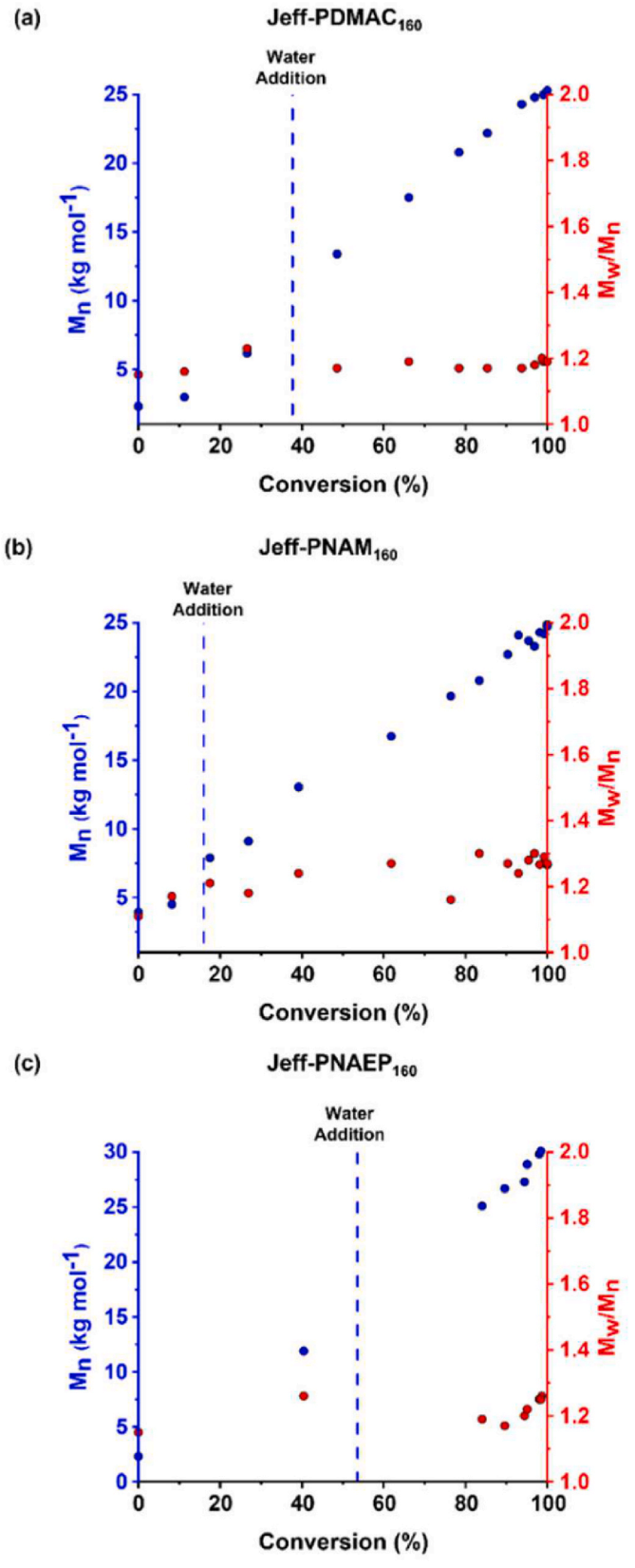

(caption on next column)

Fig. 3. M_n (blue points) and M_w/M_n (red points) data determined during the reverse sequence aqueous PISA synthesis of (a) Jeff-PDMAC$_{160}$ nanoparticles (DMF eluent), (b) Jeff-PNAM$_{160}$ nanoparticles ($CHCl_3$ eluent) and (c) Jeff-PNAEP$_{160}$ (DMF eluent) nanoparticles at 60°C via GPC analysis using a refractive index detector and calibrated using a series of poly(methyl methacrylate) standards. Initially, these RAFT polymerizations were conducted at 80 % w/w solids, with subsequent dilution to 10 % w/w solids (or 20 % w/w solids for Jeff-PNAEP$_{160}$ nanoparticles) using deoxygenated water. The corresponding intermediate monomer conversions calculated by ^{1}H NMR spectroscopy prior to dilution were (a) 38 % (DMAC), (b) 16 % (NAM) and (c) 45 % (NAEP). Final monomer conversions exceeded 99 % in each case. (For interpretation of the references to colour in this figure legend, the reader is referred to the Web version of this article.)

was added dropwise via syringe. The reaction solution was then heated to reflux and stirred continuously for 48 h. The dicyclohexylurea by-product was removed by filtration and the solvent was removed under reduced pressure using a rotary evaporator.

The resulting crude product was then purified via silica column chromatography. A 60:40 ethyl acetate/*n*-hexane eluent was used to remove the first fraction and the second fraction (containing the product) was isolated using a 90:10 dichloromethane/methanol eluent. The relevant fraction was concentrated under reduced pressure to produce a viscous orange oil. UV GPC analysis of the product confirmed that no residual CEPA was present (Fig. S2). End-group analysis was conducted via ^{1}H NMR spectroscopy: the integrated proton signal at 1.91 ppm assigned to the methyl group of the RAFT agent was compared to the integrated Jeffamine® signals assigned to the backbone at 3.47–3.65 ppm and the pendent methyl groups at 1.15 ppm. This approach indicated a mean degree of esterification of 101 ± 1 % for Jeff-TTC (see Fig. S3).

2.3.2. RAFT polymerization of a hydrophilic monomer in concentrated aqueous solution using Jeff-TTC followed by dilution at an intermediate monomer conversion

A glass vial was charged with a magnetic stirrer bar, Jeff-TTC (0.10 g, 0.04 mmol), DMAC (0.59 g, 5.91 mmol) and an aqueous AIBA solution (0.17 mL of a 50 mM solution, or 8.5 μmol AIBA; Jeff-TTC/AIBA molar ratio = 5.0) to target 80 % w/w solids. The vial was sealed with a rubber septum and a stream of nitrogen gas was used to deoxygenate the reaction mixture. After degassing for 30 min, the glass vial was immersed in a preheated oil bath set at 60°C. After 23 min, a significant increase in viscosity was observed for the reaction mixture. At this point, deoxygenated water (6.03 mL, targeting 10 % w/w solids, preheated to 60°C prior to addition) was added via syringe. An aliquot was immediately taken from the reaction mixture to determine the intermediate monomer conversion via ^{1}H NMR spectroscopy (see Table S1). The polymerization was allowed to proceed for 16 h at 60°C, before quenching by exposing the reaction mixture to air while cooling to 20°C. ^{1}H NMR studies confirmed that essentially full DMAC monomer conversion (>99 %) was achieved. For analogous syntheses using either NAEP or NAM monomers, the reagent quantities and volume of water were adjusted accordingly (see Table S1 for a summary of the details).

3. Results and discussion

According to its manufacturer, the monoamine-capped Jeffamine® M − 2005 precursor used in this study has a DP of 35 and a propylene oxide/ethylene oxide (PO/EO) molar ratio of 29/6. However, ^{1}H NMR studies of this precursor (that integrated PO and EO proton signals at 3.36–3.46 ppm and 3.47–3.65 ppm were compared to the integrated primary amine end-group protons at 1.15 ppm) suggested a mean degree of polymerization of 37 with a PO/EO molar ratio of 33/4 (see Fig. S1). Moreover, similar results were reported by Haddleton and co-workers [44].

The terminal primary amine group on this Jeffamine® precursor was

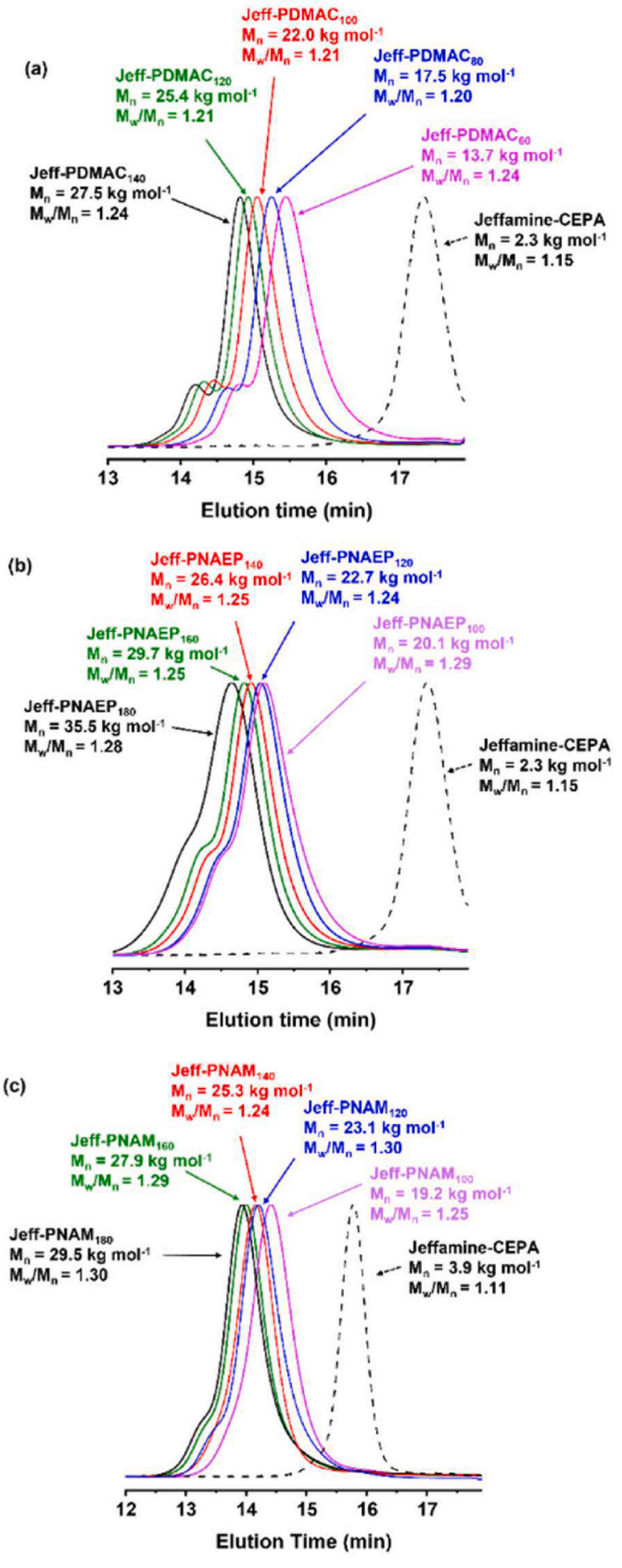

(caption on next column)

Fig. 4. GPC curves recorded using a refractive index detector for three series of Jeffamine®-based diblock copolymers prepared by reverse sequence aqueous PISA at 60°C. (a) Jeff-TTC precursor and a corresponding series of Jeff-PDMAC$_n$ (n = 60–140) diblock copolymers (DMF eluent). (b) Jeff-TTC precursor and a corresponding series of Jeff-PNAM$_n$ (n = 100–180) diblock copolymers ($CHCl_3$ eluent). (c) Jeff-TTC precursor and a corresponding series of Jeff-PNAEP$_n$ (n = 100–180) diblock copolymers (DMF eluent). Conditions: [Jeff-TTC]/[AIBA] molar ratio = 5.0. [N.B. DMF GPC curves are only shown up to an elution time of 17.9 min to omit the signal assigned to LiBr in this particular eluent (see Fig. S8)].

reacted with a carboxylic acid-functional RAFT agent (CEPA) using a well-known DCC/DMAP catalyst according to Scheme 1 to yield an intermediate denoted as Jeff-TTC [49,50]. Such amidation differs from the esterification chemistry employed for our recent reverse sequence PISA studies, whereby the same CEPA RAFT agent was reacted with either a primary or secondary monohydroxy-capped poly(ε-caprolactone) or poly(propylene oxide) precursor.[38,41] ^{1}H NMR spectroscopy was used to determine the degree of amidation and to examine whether any aminolysis of the trithiocarbonate RAFT agent had occurred [51]. Accordingly, the integrated Jeffamine® signals at 1.15 ppm and 3.47–3.65 ppm (assigned to the pendent methyl and backbone signals of the precursor respectively, see Fig. 1) were compared to that of the methyl group assigned to the RAFT agent at 1.91 ppm. This indicated a mean degree of amidation of 101 ± 1 %.

After purification, Jeff-TTC was chain-extended via reverse sequence aqueous PISA using a suitable hydrophilic vinyl monomer (e.g. DMAC, NAEP or NAM). This monomer acts as a co-solvent to ensure solubilization of the weakly hydrophobic Jeff-TTC precursor in the initial 80 % w/w reaction mixture, which comprises 5–23 % w/w Jeff-TTC, 57–75 % w/w monomer and 20 % w/w water depending on the target diblock copolymer composition (see Scheme 2). At intermediate conversion of the vinyl monomer (see Table S1) a significant increase in solution viscosity was observed. At this point, deoxygenated water (preheated to 60°C) was added to the reaction mixture. Although the time of water addition varies from experiment to experiment, our recent studies suggest that this variation results in no discernible change in either the diblock copolymer chains or the final colloidal dispersion [47]. The polymerization was allowed to proceed for 16 h at 60°C before quenching by exposing the reaction mixture to air while cooling to 20°C. ^{1}H NMR analysis indicated that essentially full monomer conversion (>99 %) was achieved under such conditions.

In our prior studies, DMAC was utilized as the sole hydrophilic monomer for such reverse sequence PISA formulations [38,41]. In the present study, six alternative hydrophilic vinyl monomers were evaluated along with DMAC: glycerol monomethacrylate (GMA), 2-(*N*-(methacryloyloxy)ethyl pyrrolidone (NMEP), 2-hydroxyethyl acrylate (HEA), 2-hydroxyethyl acrylamide (HEAC), 2-(*N*-acryloyloxyethyl pyrrolidone (NAEP), and *N*-acryloylmorpholine (NAM). However, successful reverse sequence PISA formulations could only be achieved for DMAC, NAEP and NAM when targeting a degree of polymerization (DP) for the hydrophilic block of 160. Using GMA, NMEP, HEA or HEAC enabled initial solubilization of the weakly hydrophobic Jeff-TTC precursor at 60°C but subsequent addition of deoxygenated water at intermediate conversion invariably led to these reaction mixtures becoming highly turbid. Moreover, final copolymer molecular weight distributions were relatively broad, with M_w/M_n values ranging from 1.53 to 1.84 (see Fig. S4a). Furthermore, the chain extension efficiency was only 30–60 % for such diblock copolymers (as indicated by UV GPC analysis, see Fig. S4b). This indicates that a significant proportion of the Jeff-TTC precursor did not participate in the *in situ* polymerization of the hydrophilic vinyl monomer.

After dilution to 10 % w/w at intermediate monomer conversion, the DMAC and NAM formulations produced colloidally stable aqueous dispersions of Jeffamine®-core diblock copolymer nanoparticles at essentially full conversion of the respective vinyl monomer. However,

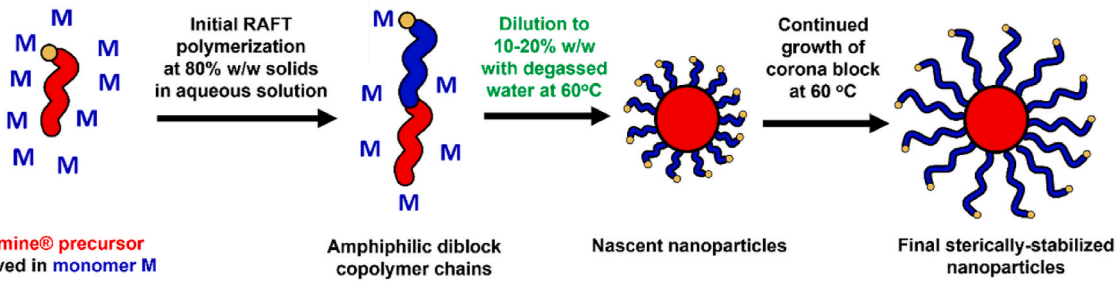

Scheme 3. Schematic cartoon of the reverse sequence PISA formulation investigated in the present study, Initially, a Jeffamine® precursor (red) bearing a trithiocarbonate end-group (yellow) is dissolved in hydrophilic monomer (blue). Subsequent polymerization produces diblock copolymer chains at 80 % w/w solids. Dilution with water produces nascent nanoparticles, with the hydrophilic coronal chains continuing to grow outwards until full monomer conversion is achieved.

macroscopic precipitation was observed under the same conditions when using NAEP. Fortunately, such colloidal instability could be avoided by dilution to 20 % w/w solids, which produced a free-flowing aqueous dispersion of nanoparticles (see Scheme 2).

To gain a better understanding of the kinetics of such polymerizations, the reaction mixture was periodically sampled both before and after dilution with water and such aliquots were subjected to ^{1}H NMR and GPC analysis. ^{1}H NMR spectroscopy indicated that the fastest rate of polymerization was achieved for the NAM formulation. In this case, water was added after 8 min (corresponding to 16 % NAM conversion) and full monomer conversion was achieved within 105 min (see Fig. 2). When DMAC was employed as the hydrophilic monomer, water was added after 23 min (DMAC conversion = 38 %) and full conversion was achieved within 3 h. Finally, water was added after 23 min (45 % conversion) when using NAEP, with full conversion being achieved within 4 h at 60 °C.

In all cases, GPC analysis indicated a linear increase in number-average molecular weight (M_n) with conversion (see Fig. 3). Moreover, efficient chain extension was observed (see Fig. S5) and relatively narrow molecular weight distributions were obtained ($M_w/M_n < 1.30$ in all cases), suggesting that good RAFT control can be achieved during these reverse sequence aqueous PISA syntheses [52–54].

After establishing that reasonably well-controlled polymerizations could be achieved when using DMAC, NAM and NAEP, a series of such Jeffamine®-based diblock copolymers was prepared (see Fig. 4). When using DMAC, UV GPC analysis ($\lambda = 305$ nm, which corresponds to the absorption maximum for the trithiocarbonate chain-ends) confirmed very high chain extension efficiencies (>96 %, see Fig. S6) with minimal evidence for unreacted Jeff-TTC chains. However, a high molecular weight peak/shoulder is also observed in the GPC trace. Moreover, the molecular weight of this secondary feature is always approximately double that of the main peak, which suggests some degree of termination by combination (i.e. chain-chain coupling). One reviewer of this manuscript has suggested that the probability of such chain-chain coupling may be enhanced by the outward growth nature of the steric stabilizer chains, as exemplified in Scheme 3. We agree that this is a plausible explanation and note that similar chain-chain coupling is well-documented for the synthesis of star polymers in the literature [55,56].

The same technique indicated significantly less efficient reverse sequence PISA syntheses when using either NAM or NAEP. A linear relationship between M_n and target DP was observed in each case (see Fig. S7) but tailing of UV GPC traces recorded for the Jeff-PNAM diblock copolymer chains suggested the presence of approximately 7–9% unreacted Jeff-TTC chains. Furthermore, chain extension efficiencies were reduced to 70–84 % for NAEP-based formulations. This implies that up to 30 % of the Jeff-TTC precursor remained unreacted in such syntheses (see Fig. S6). It is perhaps worth emphasizing that such chain extension problems are not discernible in the corresponding refractive index GPC curves (see Fig. 4).

DLS and TEM studies were performed to examine the nanoparticle size and morphology. Unimodal populations were observed in all cases for the Jeff-PDMAC and Jeff-PNAEP nanoparticles, with z-average diameters ranging from 196 to 245 nm and 145–212 nm respectively (see Fig. 5a and b). In contrast, targeting a PNAM DP of 100, 160 or 180 produced multimodal size distributions for Jeff-PNAM nanoparticles, with a major population at 140–160 nm while targeting a PNAM DP of 140 produced a relatively broad size distribution. On the other hand, a unimodal population of 163 nm was obtained when targeting a PNAM DP of 120 (see Fig. 5c). This latter observation suggests that further optimization is required for such NAM-based reverse sequence aqueous PISA formulations.

For a series of Jeff-PDMAC$_x$ diblock copolymers, DLS studies indicated the formation of larger particles when targeting progressively lower PDMAC DPs. This is consistent with the accepted theory of diblock copolymer self-assembly, as outlined by Mai and Eisenberg [57]. Moreover, similar experimental findings have been recently reported by Warren and co-workers for a series of diblock copolymers in which the DP of the steric stabilizer block was varied from 47 to 143 while the core-forming block was held constant at 400 [58].

TEM studies proved to be technically challenging because the glass transition temperature (T_g) of the core-forming Jeffamine® M − 2005 block is around −70°C [44]. Nevertheless, TEM images were obtained for Jeff-PDMAC$_{120}$, Jeff-PNAEP$_{120}$ and Jeff-PNAM$_{120}$ nanoparticles, confirming a polydisperse spherical morphology in each case (see Fig. 6). Number-average diameters of 94 ± 27 nm, 92 ± 32 nm and 96 ± 46 nm nm respectively were estimated from such images. Presumably, the relatively high T_g value of around 120°C for the PDMAC chains [59], 140°C for the PNAM chains [60] and 20°C for the PNAEP chains [61] raises the effective T_g of the Jeffamine® core-forming chains, which hence enables TEM analysis of the diblock copolymer nanoparticles.

TEM is only sensitive to the nanoparticle cores because the steric stabilizer chains are of negligible thickness under the ultrahigh vacuum conditions required for electron microscopy. In contrast, DLS 'sees' the whole nanoparticle (e.g. the Jeffamine® core plus the solvated steric stabilizer coronal chains). Moreover, the latter technique is biased towards larger nanoparticles for particle size distributions of finite width. These factors account for the apparent discrepancy between the TEM and DLS data. TEM studies were also performed on dried aqueous dispersions of Jeff-PDMAC$_{140}$ and Jeff-PDMAC$_{60}$ nanoparticles. Inspecting the TEM images shown in Fig. 7 and Fig. S9, polydisperse spheres were observed in both cases. Number-average diameters of 84 ± 31 nm and 285 ± 139 nm were estimated for the former and latter nanoparticles, respectively.

For Jeff-PDMAC$_{120}$, Jeff-PNAEP$_{120}$ and Jeff-PNAM$_{120}$ nanoparticles, zeta potentials were determined to be close to zero from pH 4 to pH 9, (see Fig. 8). This is consistent with the non-ionic nature of the PDMAC,

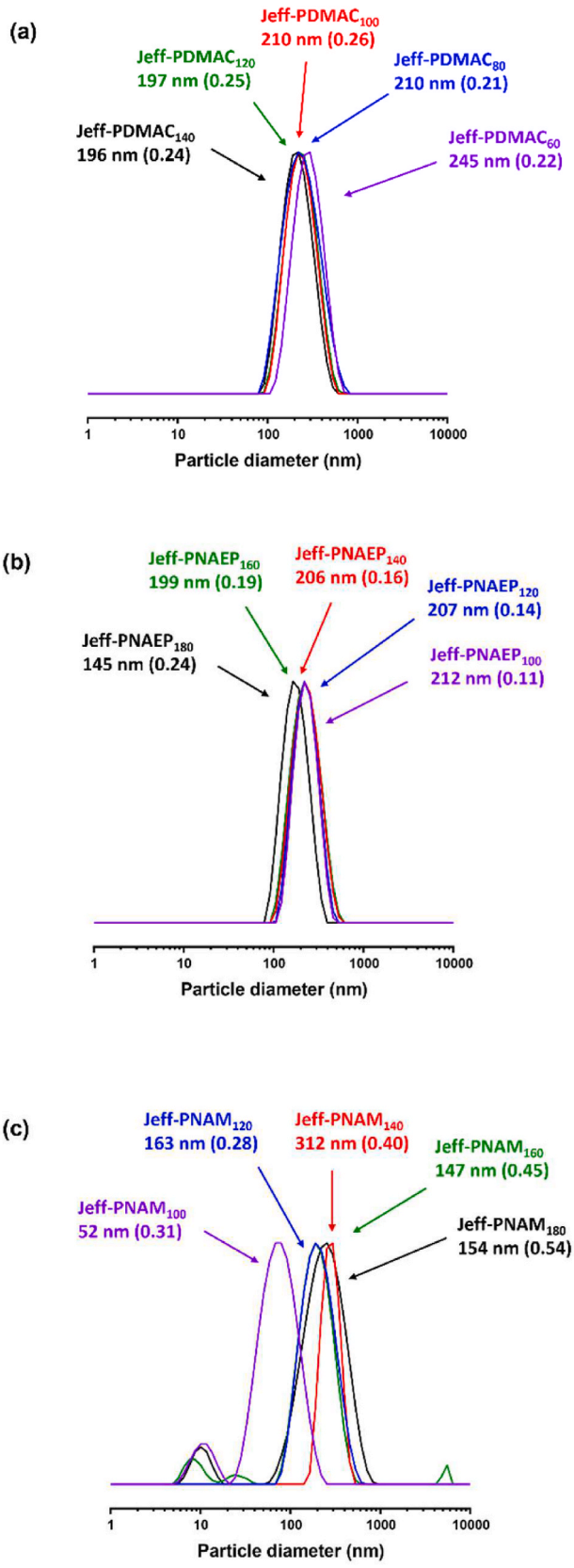

Fig. 5. DLS particle size distributions recorded for 1.0 % w/w aqueous dispersions of (a) Jeff-PDMAC$_{60\text{-}140}$, (b) Jeff-PNAEP$_{100\text{-}180}$ and (c) Jeff-PNAM$_{100\text{-}180}$ nanoparticles prepared via reverse sequence aqueous PISA at 60°C.

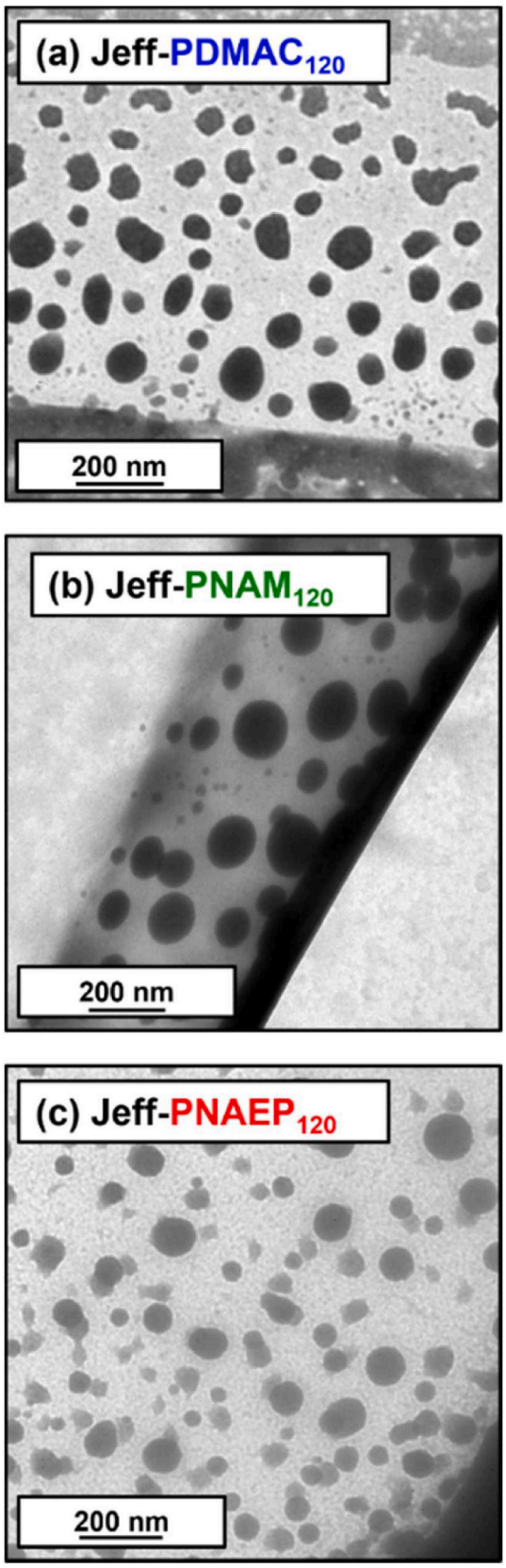

Fig. 6. Representative TEM images recorded after drying dilute aqueous dispersions of (a) Jeff-PDMAC$_{120}$ nanoparticles, (b) Jeff-PNAM$_{120}$ nanoparticles and (c) Jeff-PNAEP$_{120}$ nanoparticles.

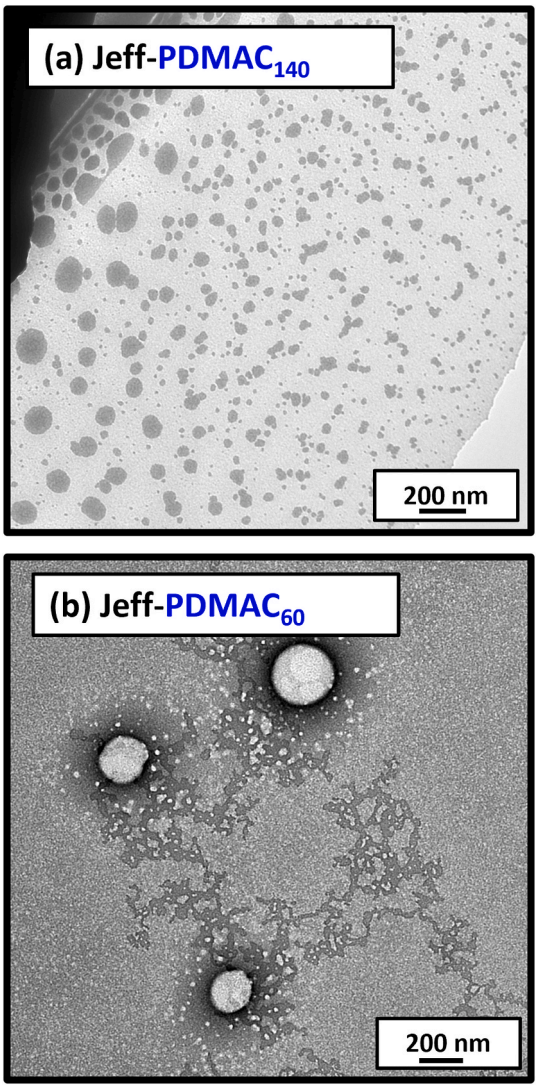

Fig. 7. Representative TEM images recorded after drying dilute aqueous dispersions of (a) Jeff-PDMAC$_{140}$ nanoparticles and (b) Jeff-PDMAC$_{60}$ nanoparticles.

PNAEP and PNAM steric stabilizer chains. Thus the aqueous electrophoresis data suggest that the colloidal stability observed for these nanoparticles in aqueous media is simply the result of steric stabilization, rather than charge stabilization.

4. Conclusions

Our original reverse sequence PISA protocol [38] has been expanded to include a Jeffamine®-based precursor. The higher solubility of this precursor enables these syntheses to be performed at only 60°C, rather than 80°C. Moreover, such wholly aqueous formulations enable two new hydrophilic vinyl monomers (NAM and NAEP) to be employed, in addition to the original DMAC monomer. In each case, a linear evolution in number-average molecular weight with conversion and relatively low copolymer dispersities ($M_w/M_n < 1.30$) were observed when targeting a DP of 160 for the hydrophilic block, suggesting good RAFT control. However, UV GPC studies confirmed significantly higher chain extension efficiencies for DMAC polymerizations compared to reverse sequence PISA syntheses performed using either NAM or NAEP. TEM studies indicated the formation of polydisperse spherical nanoparticles in all cases and DLS studies reported hydrodynamic z-average diameters ranging from 145 nm to 245 nm. Unimodal populations could be

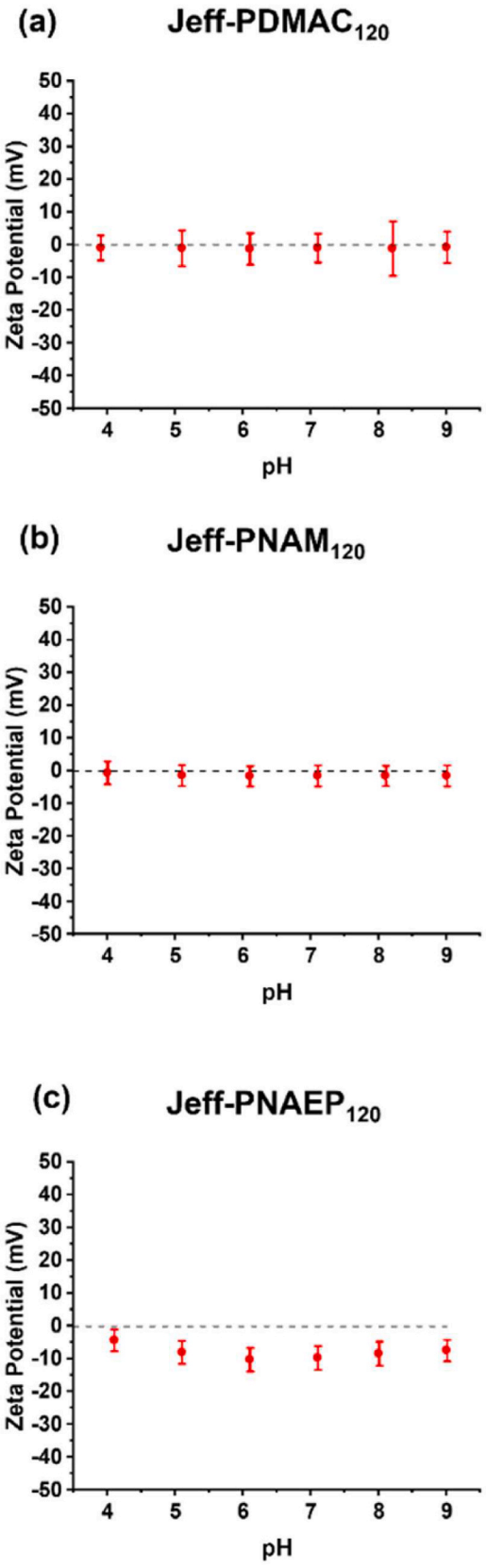

Fig. 8. Zeta potential vs. pH curves obtained for 1.0 % w/w aqueous dispersions of (a) Jeff-PDMAC$_{120}$ nanoparticles, (b) Jeff-PNAM$_{120}$ nanoparticles and (c) Jeff-PNAEP$_{120}$ nanoparticles.

obtained for some (but not all) reverse sequence PISA formulations. Finally, aqueous electrophoresis data suggested a steric stabilization mechanism for these Jeffamine®-core nanoparticles.

CRediT authorship contribution statement

Matthew A.H. Farmer: Writing – review & editing, Writing – original draft, Visualization, Validation, Methodology, Investigation, Formal analysis, Data curation. **Osama M. Musa:** Supervision, Resources, Project administration, Funding acquisition. **Steven P. Armes:** Writing – review & editing, Writing – original draft, Supervision, Project administration, Methodology, Funding acquisition, Conceptualization.

Declaration of competing interest

The authors declare the following financial interests/personal relationships which may be considered as potential competing interests:

Steven Armes reports financial support was provided by Ashland Specialty Ingredients GP. Steven Armes reports financial support was provided by Engineering and Physical Sciences Research Council. Osama Musa reports a relationship with Ashland Specialty Ingredients GP that includes: employment. Matthew Farmer, Osama Musa, Steven Armes has patent pending to Ashland Speciality Ingredients GP. If there are other authors, they declare that they have no known competing financial interests or personal relationships that could have appeared to influence the work reported in this paper.

Data availability

Data will be made available on request.

Acknowledgements

EPSRC is thanked for funding a CASE PhD studentship for the first author and for an Established Career Particle Technology Fellowship (EP/R003009) for S. P. Armes. Ashland Specialty Ingredients (Bridgewater, New Jersey, USA) is thanked for financial support of this PhD project and for permission to publish this work.

Appendix A. Supplementary data

Supplementary data to this article can be found online at https://doi.org/10.1016/j.polymer.2024.127474.

References

[1] J. Rieger, Macromol. Rapid Commun. 36 (2015) 1458–1471.
[2] S.L. Canning, G.N. Smith, S.P. Armes, Macromolecules 49 (2016) 1985–2001.
[3] B. Charleux, G. Delaittre, J. Rieger, F. D'Agosto, Macromolecules 45 (2012) 6753–6765.
[4] N.J. Warren, S.P. Armes, J. Am. Chem. Soc. 136 (2014) 10174–10185.
[5] N.J.W. Penfold, J. Yeow, C. Boyer, S.P. Armes, ACS Macro Lett. 8 (2019) 1029–1054.
[6] S. Dong, W. Zhao, F.P. Lucien, S. Perrier, P.B. Zetterlund, Polym. Chem. 6 (2015) 2249–2254.
[7] F. D'Agosto, J. Rieger, M. Lansalot, Angew. Chem. Int. Ed. 59 (2020) 8368–8392.
[8] C. Grazon, J. Rieger, N. Sanson, B. Charleux, Soft Matter 7 (2011) 3482–3490.
[9] G. Wang, M. Schmitt, Z. Wang, B. Lee, X. Pan, L. Fu, J. Yan, S. Li, G. Xie, M. R. Bockstaller, K. Matyjaszewski, Macromolecules 49 (2016) 8605–8615.
[10] G. Delaittre, J. Nicolas, C. Lefay, M. Save, B. Charleux, Chem. Commun. (2005) 614–616.
[11] A. Blanazs, J. Madsen, G. Battaglia, A.J. Ryan, S.P. Armes, J. Am. Chem. Soc. 133 (2011) 16581–16587.
[12] E.E. Brotherton, F.L. Hatton, A.A. Cockram, M.J. Derry, A. Czajka, E.J. Cornel, P. D. Topham, O.O. Mykhaylyk, S.P. Armes, J. Am. Chem. Soc. 141 (2019) 13664–13675.
[13] J. Lesagedelahaye, X. Zhang, I. Chaduc, F. Brunel, M. Lansalot, F. D'Agosto, Angew. Chem. Int. Ed. 55 (2016) 3739–3743.
[14] S.J. Byard, C.T. O'Brien, M.J. Derry, M. Williams, O.O. Mykhaylyk, A. Blanazs, S. P. Armes, Chem. Sci. 11 (2020) 396–402.
[15] C.A. Figg, R.N. Carmean, K.C. Bentz, S. Mukherjee, D.A. Savin, B.S. Sumerlin, Macromolecules 50 (2017) 935–943.
[16] Y. Zhang, G. Han, M. Cao, T. Guo, W. Zhang, Macromolecules 51 (2018) 4397–4406.
[17] J. Rieger, G. Osterwinter, C. Bui, F. Stoffelbnach, B. Charleux, Macromolecules 42 (2009) 5518–5525.
[18] S. Sugihara, A.H. Ma'Radzi, S. Ida, S. Irie, T. Kikukawa, Y. Maeda, Polymer 76 (2015) 17–24.
[19] Z. An, Q. Shi, W. Tang, C.K. Tsung, C.J. Hawker, G.D. Stucky, J. Am. Chem. Soc. 129 (2007) 14493–14499.
[20] C.A. Figg, A. Simula, K.A. Gebre, B.S. Tucker, D.M. Haddleton, B.S. Sumerlin, Chem. Sci. 6 (2015) 1230–1236.
[21] L. Houillot, C. Bui, M. Save, B. Charleux, C. Farcet, C. Moire, J.A. Raust, I. Rodriguez, Macromolecules 40 (2007) 6500–6509.
[22] M.J. Derry, L.A. Fielding, S.P. Armes, Prog. Polym. Sci. 52 (2016) 1–18.
[23] Q. Zhang, S. Zhu, ACS Macro Lett. 4 (2015) 755–758.
[24] E.R. Jones, M. Semsarilar, P. Wyman, M. Boerakker, S.P. Armes, Polym. Chem. 7 (2016) 851–859.
[25] R.R. Gibson, A. Fernyhough, O.M. Musa, S.P. Armes, Polym. Chem. 12 (2021) 2165–2174.
[26] J. Jennings, M. Beija, J.T. Kennon, H. Willcock, R.K. O'Reilly, S. Rimmer, S. M. Howdle, Macromolecules 46 (2013) 6843–6851.
[27] C. György, S.P. Armes, Angew. Chem. Int. Ed. 62 (2023) e202308372.
[28] A. Stiti, A.M. Cenacchi Pereira, S. Lecommandoux, D. Taton, Angew. Chem. Int. Ed. 62 (2023) e202305945.
[29] K. Mattsson, E.V. Johnson, A. Malmendal, S. Linse, L.A. Hansson, T. Cedervall, Sci. Rep. 7 (2017) 11452.
[30] M. Eriksen, L.C.M. Lebreton, H.S. Carson, M. Thiel, C.J. Moore, J.C. Borerro, F. Galgani, P.G. Ryan, J. Reisser, PLoS One 9 (2014) e111913.
[31] K. Duis, A. Coors, Environ. Sci. Eur. 28 (2016) 1–25.
[32] P. Galanopoulo, N. Gil, D. Gigmes, C. Lefay, Y. Guillaneuf, M. Lages, J. Nicolas, F. D'Agosto, M. Lansalot, Angew. Chem. Int. Ed. 62 (2023) e202302093.
[33] E. Guégain, C. Zhu, E. Giovanardi, J. Nicolas, Macromolecules 52 (2019) 3612–3624.
[34] C. Zhu, J. Nicolas, Polym. Chem. 12 (2021) 594–607.
[35] C. Zhu, S. Denis, J. Nicolas, Chem. Mater. 34 (2022) 1875–1888.
[36] C. Grazon, P. Salas-Ambrosio, E. Ibarboure, A. Buol, E. Garanger, M.W. Grinstaff, S. Lecommandoux, C. Bonduelle, Angew. Chem. Int. Ed. 59 (2020) 622–626.
[37] C. Grazon, P. Salas-Ambrosio, S. Antoine, E. Ibarboure, O. Sandre, A.J. Clulow, B. J. Boyd, M.W. Grinstaff, S. Lecommandoux, C. Bonduelle, Polym. Chem. 12 (2021) 6242–6251.
[38] M.A.H. Farmer, O.M. Musa, S.P. Armes, Angew. Chem. Int. Ed. 62 (2023) e202309526.
[39] Q. Shi, Y. Chen, J. Yang, J. Yang, Chem. Commun. 57 (2021) 11390–11393.
[40] J. Jiang, X. Zhang, Z. Fan, J. Du, ACS Macro Lett. 8 (2019) 1216–1221.
[41] M.A.H. Farmer, O.M. Musa, I. Haug, S. Naumann, S.P. Armes, Macromolecules 57 (2024) 317–327.
[42] T.J. Neal, N.J.W. Penfold, S.P. Armes, Angew. Chem. Int. Ed. 61 (2022) e202207376.
[43] H. Buksa, T.J. Neal, S. Varlas, S.J. Hunter, O.M. Musa, S.P. Armes, Macromolecules 56 (2023) 4296–4306.
[44] J. Zhang, E. Liarou, J. Town, Y. Li, A.M. Wemyss, D.M. Haddleton, Polym. Chem. 11 (2020) 5534–5541.
[45] Y. Cai, Y. Tang, S.P. Armes, Macromolecules 37 (2004) 9728–9737.
[46] W. Agut, A. Brulet, D. Taton, S. Lecommandoux, Langmuir 23 (2007) 11526–11533.
[47] M.A.H. Farmer, O.M. Musa, S.P. Armes, J. Am. Chem. Soc. 146 (2024) 16926–16934.
[48] M. Danial, S. Telwatte, D. Tyssen, S. Cosson, G. Tachedjian, G. Moad, A. Postma, Polym. Chem. 7 (2016) 7477–7487.
[49] B. Neises, W. Steglich, Angew. Chem. Int. Ed. 17 (1978) 522–524.
[50] A.P. Lopez-Oliva, N.J. Warren, A. Rajkumar, O.O. Mykhaylyk, M.J. Derry, K.E. B. Doncom, M.J. Rymaruk, S.P. Armes, Macromolecules 48 (2015) 3547–3555.
[51] X.P. Qiu, F.M. Winnik, Macromol. Rapid Commun. 27 (2006) 1648–1653.
[52] J. Chiefari, Y.K.B. Chong, F. Ercole, J. Krstina, J. Jeffery, T.P.T. Le, R.T. A. Mayadunne, G.F. Meijs, C.L. Moad, G. Moad, E. Rizzardo, S.H. Thang, Macromolecules 31 (1998) 5559–5562.
[53] S. Perrier, Macromolecules 50 (2017) 7433–7447.
[54] D.J. Keddie, Chem. Soc. Rev. 43 (2014) 496–505.
[55] K. Ohno, B. Wong, D.M. Haddleton, J. Polym. Sci. Part A polym. Chem. 39 (2001) 2206–2214.
[56] D. Boschmann, P. Vana, Macromolecules 40 (2007) 2683–2693.
[57] Y. Mai, A. Eisenberg, Chem. Soc. Rev. 41 (2012) 5969–5985.
[58] J.D. Guild, S.T. Knox, S.B. Burholt, E.M. Hilton, N.J. Terrill, S.L.M. Schroeder, N. J. Warren, Macromolecules 56 (2023) 6426–6435.
[59] T.P. Yang, E.M. Pearce, T.K. Kwei, N.L. Yang, Macromolecules 22 (1989) 1813–1818.
[60] J.Z. Yi, S.H. Goh, Polymer 43 (2002) 4515–4522.
[61] O.J. Deane, O.M. Musa, A. Fernyhough, S.P. Armes, Macromolecules 53 (2020) 1422–1434.